

## Statics, metastable states, and barriers in protein folding: A replica variational approach

Shoji Takada and Peter G. Wolynes

*School of Chemical Sciences, University of Illinois, Urbana, Illinois 61801*

(Received 26 February 1996; revised manuscript received 15 August 1996)

Protein folding is analyzed using a replica variational formalism to investigate some free energy landscape characteristics relevant for dynamics. A random contact interaction model that satisfies the minimum frustration principle is used to describe the coil-globule transition (characterized by  $T_{CG}$ ), glass transitions (by  $T_A$  and  $T_K$ ), and folding transition (by  $T_F$ ). Trapping on the free energy landscape is characterized by two characteristic temperatures, one dynamic ( $T_A$ ) and the other static [ $T_K$  ( $T_A > T_K$ )], which are similar to those found in mean field theories of the Potts glass. (i) Above  $T_A$ , the free energy landscape is monotonous and the polymer is melted both dynamically and statically. (ii) Between  $T_A$  and  $T_K$ , the melted phase is still dominant thermodynamically, but frozen metastable states, exponentially large in number, appear. (iii) A few lowest minima become thermodynamically dominant below  $T_K$ , where the polymer is totally frozen. In the temperature range between  $T_A$  and  $T_K$ , barriers between metastable states are shown to grow with decreasing temperature, suggesting super-Arrhenius behavior in a sufficiently large system. Due to evolutionary constraints on fast folding, the folding temperature  $T_F$  is expected to be higher than  $T_K$ , but may or may not be higher than  $T_A$ . Diverse scenarios of the folding kinetics are discussed based on phase diagrams that take into account the dynamical transition, as well as the static ones. [S1063-651X(97)11304-6]

PACS number(s): 87.15.-v, 61.41.+e, 64.70.Pf

### I. INTRODUCTION

In recent years the problem of protein folding, namely, how a biological molecule spontaneously organizes itself under appropriate thermodynamic conditions, has become a fertile field of investigation for statistical physics [1–4]. The conceptual difficulty of finding the global free energy minimum, or native structure, reliably in a short amount of time, the so-called *Levinthal's paradox* [5], has come to be understood as being related to the problem of broken ergodicity in glassy systems [6]. In the modern version of the paradox, however, it is not the size of the configurational search alone that is relevant but rather the topography of the free energy landscape. The size of the free energy barriers between the metastable states of a finite size heteropolymer determines the local rate of exploration of the free energy landscape. In addition, the global topography, in particular, whether there is an energetic bias funneling [7] the molecule toward a native structure, is also important to understand the folding rate.

The earliest analytical approach to the problem captured these two aspects of the problem—the multiple minima problem and the guiding forces with the simplest description of the free energy landscape [8,9]. The ruggedness of the free energy surface was modeled by the random energy model (REM) [10]. The REM is the simplest model of a system that, like a spin glass, is frustrated through the conflict of many competing randomly chosen interactions. A sufficiently large system with this free energy landscape was shown to possess a Levinthal paradox in its folding. More precisely, at a characteristic glass transition temperature  $T_K$ , while the system may thermodynamically prefer to be in a unique configuration, the time to search for it would scale exponentially in the system size. (“ $K$ ” of  $T_K$  denotes Kauzmann, who attracted notice to the entropy crisis as the origin of the glass transition [11]. See below for more details.) Proteins are finite, however, so it is a quantitative issue whether

such a system can fold on relevant biological time scales. Buttressed by this asymptotic argument, but also calling upon observed regularities in protein structure, Bryngelson and Wolynes argued that most proteins are not random but additionally satisfy a principle of minimal frustration, so that conflicts in attempting to satisfy individual interactions are less than expected, allowing a transition to a unique configuration at a folding temperature  $T_F$  higher than  $T_K$ . The coherent part of the interactions could be taken into account in the statics by introducing a conventional order parameter for folding, as in mean field theory. For a small system this order parameter can also act as an approximate global reaction coordinate for describing the self-organization process [9]. This relatively simple framework can be elaborated to take into account additional order parameters for folding, such as local secondary structure formation [12] and recently correlations in the free energy landscape [13]. The framework and the resulting mechanistic scenarios are also quite useful for organizing the discussions of many experiments [1].

Another significant thread in the statistical physics of protein folding has been provided by theories that use the replica technology of spin glass theory [6] along with polymer physics to understand the free energy landscape [14–19]. Garel and Orland [14], as well as Shakhnovich and Gutin [15], studied random heteropolymers using the traditional polymeric virial expansion Hamiltonian of a connected chain incorporating a Gaussian random pair interaction. These workers showed the connection of the random heteropolymer thermodynamics with the phase transition of Potts glass [20]. Qualitatively this was not entirely unexpected because a wide range of frustrated random systems without special symmetries falls in this universality class, which also includes the REM model [20–23]. This work was relevant to the ruggedness issues but not to the problem of guiding forces. Soon after this work, Sasai and Wolynes dealt with three aspects—polymeric interaction, ruggedness of free energy landscape, and results of evolution—in one model [16].

They employed a variational approach modeled on Feynman's polaron theory [24] in the replica space to analyze the associative memory Hamiltonian [25]. (i) This model has explicit chain connectivity, (ii) the target structure, i.e., the native structure, included in the memory set (or data base) provides a route to incorporate the role of principle of minimal frustration, while (iii) memories other than the target induce ruggedness in the free energy landscape. Very recently, Ramanathan and Shakhnovich shed light on effects of the evolutionary constraint of minimal frustration in more detail [17]. Instead of assuming the pronounced energy gap *a priori*, they represented evolution as a process that yields sequences distributed according to a Boltzmann distribution for a fixed target structure. Their theory shows that it is possible to have an energy gap large enough to stabilize the native structure only by choosing the sequence appropriately, although it is not clear if nature actually used such a sequence selection mechanism or not. An alternative route to minimal frustration called "imprinting" has also been discussed by Pande *et al.* [18], which finally gives almost same result as [17].

Levinthal's paradox makes it clear that the conceptual issues of the folding problem revolve on *kinetics* in at least a semiquantitative fashion. Theory and many simulations [26,27] in concurrence suggest that real proteins fold below their folding temperature  $T_F$  but somewhat above the (static) glass phase transition temperature  $T_K$ . Thus, to understand the kinetics of folding, a microscopic description of the free energy landscape above  $T_K$  is indispensable. Is the effective free energy landscape monotonous and smooth above  $T_K$ ? We claim no. Even above  $T_K$  there are a number of local minima lasting many vibrational periods (Rouse relaxation times) in the free energy landscape. Although the variational solution corresponding with the melt phase dominates the formal Boltzmann average, actually a protein is dynamically trapped and feels some of the ruggedness of the free energy landscape and thus kinetics would strongly be affected by the presence of local minima. Then the next question that arises concerns the barrier heights between these local minima because these barrier heights determine the kinetics. We show that barrier heights grow with decreasing temperature until  $T_K$  is reached, which directly leads us to the super-Arrhenius activation behavior in this temperature regime.

To make this analysis we utilize recently developed ideas in the spin glass theory, especially for the Potts-type spin glass [22,23,28,29]. In a series of papers, Kirkpatrick, Thirumalai, and Wolynes, working on models of structural glasses [21],  $p$ -spin interaction model glasses ( $p > 2$ ) [22], and the Potts glasses with more than four components [23], made the following observations. (i) The phase transition temperature  $T_A$  obtained by the dynamical theory, i.e., mode-mode coupling theory based on Langevin dynamics, is higher than the  $T_K$  obtained by the static theory, i.e., the ordinary replica method. (ii) As temperature decreases, starting from the paramagnetic phase, solutions of the Thouless-Anderson-Palmer (TAP) equations [30] (except the paramagnetic one) appear exactly at  $T_A$  (see Fig. 1). (iii) For  $T_A > T > T_K$ , many metastable states are separated by high barriers and therefore have a long lifetime. Thus activated transport is the typical picture in this range ("A" of  $T_A$  denotes "activation"). (iv) The overlap order parameter  $q$  in the same group of 1 level

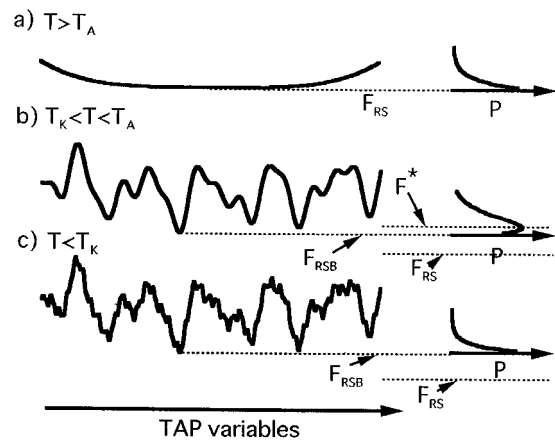


FIG. 1. Schematic view of the TAP free energy landscape with the Boltzmann distribution plots. (a) Above  $T_A$ , the free energy landscape is monotonous. (b) At  $T_A > T > T_K$ , the free energy landscape has a number of minima, and a collection of metastable states contributes to the Boltzmann average, which corresponds to the replica symmetric solution  $F_{RS}$ . (c) Below  $T_K$ , the free energy landscape has a number of minima but only a few lowest states dominate the Boltzmann average, which is calculated by the RSB solution  $F_{RSB}$ .

replica symmetry breaking (RSB) takes a discontinuous jump at  $T_K$ , which reminds us of a first order phase transition in the order parameter, but the transition looks second order in that, thermodynamically, there is no latent heat. (This was known and well understood in the case of REM.) They called this class of phase transitions *random first order phase transitions*. Crisanti and Sommers found essentially the same behavior in the  $p$ -spin spherical model [28], which buttresses the case that this type of behavior, very different from that of the Sherrington-Kirkpatrick model, is quite universal for systems without inversion symmetry. Using the  $p$ -spin spherical model Kurchan, Parisi, and Virasoro succeeded in describing the metastable states in greater detail and the barriers between them in the replica formalism [29], which we use in this paper. This formalism for describing metastable states has some forbidding aspects. Like the equilibrium replica technique, there are steps involving analytical continuation to apparently nonphysical values of replica number. More work to clarify the techniques would be welcome, but the physical content seems very much in keeping with a transition driven by configurational entropy. Barrier heights are determined by a competition between the number of available states and the energetic advantage that a polymer can achieve in a particular lower minimum. The results on barrier heights are the main focus of this paper.

In this paper we employ the contact interaction model used in [15] with the principle of minimal frustration implemented at the level of [16]. Methodologically, we rely on the replica variational approach of Sasai and Wolynes, but extend the interpretation to the level of Kurchan, Parisi, and Virasoro [29] for metastable states and barriers. These methods are summarized in Sec. II. In Sec. III, we introduce some approximations so that we can derive expressions for the free energy in as simple a form as possible. These expressions are used in Sec. IV to locate the phase transitions between different phases. We derive explicit expressions for four phase transition temperatures, the coil-globule transition tempera-

ture  $T_{CG}$ , the folding temperature  $T_F$ , the dynamical glass temperature  $T_A$ , and the static glass temperature  $T_K$ . In particular, the ruggedness of the free energy landscape is characterized by two critical temperatures of freezing,  $T_A$  and  $T_K$ , as in the case of Potts glass. In Sec. V we draw phase diagrams with fairly diverse states and discuss several scenarios of the folding kinetics, which can be thought of as a refined version of the scenarios given in [1]. Complete but somewhat messy expressions for the free energy are given in the Appendix.

## II. REPLICA VARIATIONAL APPROACH

### A. Model

The model we present here, while different from that used by Sasai and Wolynes [16], is motivated by it. Our main goal in this section is to show how a model with short range (in space) interaction can be treated with the same formalism as the long range associative memory model.

As a simple model of protein, we start with a standard beads-type Hamiltonian, which includes the interaction between monomers in the form of the virial expansion,

$$H = k_B T \sum_i \frac{(\mathbf{r}_{i+1} - \mathbf{r}_i)^2}{2a^2} + \frac{v}{2} \sum_{i \neq j} b_{ij} \delta(\mathbf{r}_i - \mathbf{r}_j) + c \frac{v^2}{6} \sum_{i \neq j \neq k} \delta(\mathbf{r}_i - \mathbf{r}_j) \delta(\mathbf{r}_j - \mathbf{r}_k), \quad (1)$$

where  $\mathbf{r}_i$  represents  $\alpha$  carbon of each amino acid ( $i = 1, \dots, N$ ),  $a$  is the Kuhn length [31],  $v$  represents finite resolution of space (see below), and  $b_{ij}$  and  $c$  are the second and third virial coefficients, respectively. Depending on the type of amino acids, individual  $b_{ij}$  have apparently random values, whose distribution will be given below. We assume the spatial resolution is  $v^{1/3}$  and so any function is smeared out within this scale. Therefore,  $\delta(\mathbf{0}) = v^{-1}$ . The above Hamiltonian itself is directly suitable to the random heteropolymer, as was used in [15].

Since a protein can fold because of its specific sequence, it is indispensable to incorporate the principle of minimal frustration, as was mentioned in the Introduction. The key idea here is that the energy of ground state, which corresponds to the target structure defined by amino acid positions  $\{\mathbf{r}_i^T\}$  of the native state, depends strongly on the specific sequence of amino acids, while properties of non-native structures can well be modeled by the random interaction between amino acids. In other words, the energy of the native structure is non-self-averaging, while most others that are structurally unrelated are self-averaging. This is supported by numerical enumeration of all the compact states in the lattice 27-mer [27]. Using a measure of nativeness [50],

$$q = \frac{v}{N} \sum_i \delta(\mathbf{r}_i - \mathbf{r}_i^T), \quad (2)$$

we rewrite the above Hamiltonian separating the non-self-averaging part from the others,

$$H = k_B T \sum_i \frac{(\mathbf{r}_{i+1} - \mathbf{r}_i)^2}{2a^2} + (1-q) \frac{v}{2} \sum_{i \neq j} b_{ij} \delta(\mathbf{r}_i - \mathbf{r}_j) + (1-q)c \frac{v^2}{6} \sum_{i \neq j \neq k} \delta(\mathbf{r}_i - \mathbf{r}_j) \delta(\mathbf{r}_j - \mathbf{r}_k) + qE^T, \quad (3)$$

where

$$qE^T = \frac{v}{N} \sum_i \delta(\mathbf{r}_i - \mathbf{r}_i^T) \left[ \frac{v}{2} \sum_{i \neq j} b_{ij} \delta(\mathbf{r}_i - \mathbf{r}_j) + c \frac{v^2}{6} \sum_{i \neq j \neq k} \delta(\mathbf{r}_i - \mathbf{r}_j) \delta(\mathbf{r}_j - \mathbf{r}_k) \right]. \quad (4)$$

Here we introduce an approximation,

$$qE^T \simeq \frac{v}{N} \sum_i \delta(\mathbf{r}_i - \mathbf{r}_i^T) \left[ \frac{v}{2} \sum_{i \neq j} b_{ij} \delta(\mathbf{r}_i^T - \mathbf{r}_j^T) + c \frac{v^2}{6} \sum_{i \neq j \neq k} \delta(\mathbf{r}_i^T - \mathbf{r}_j^T) \delta(\mathbf{r}_j^T - \mathbf{r}_k^T) \right], \quad (5)$$

which is exact either when the system is in the native structure or when the system is totally uncorrelated to the native structure. In Eq. (3), the second and third terms are assumed to be self-averaging, while the last term is non-self-averaging. After the non-self-averaging term representing minimal frustration of the target structure is taken into account, the interaction energies  $b_{ij}$  in Eq. (3) may be modeled, as was mentioned, by Gaussian random variables with probability distribution,

$$P(b_{ij}) = (2\pi b^2)^{-1/2} \exp[-(b_{ij} - b_0)^2 / 2b^2]. \quad (6)$$

Note that we do *not* take an average of  $b_{ij}$  in Eq. (5), which are thought as sequence specific. Equations (3), (5), and (6) define the model, in which parameters  $T$ ,  $b_0$ ,  $b$ , and  $E^T$  play central roles.

Here, we should bear in mind that the virial expansion is, as is well-known, good for extended states such as the random coil state but not very accurate for highly collapsed states, in which we are mainly interested. Thus, the present thermodynamic description of the radius of polymer, in particular, may not be particularly accurate.

### B. Replica variational formalism and mean field approximation

We summarize the variational polaron approach in replica space used earlier [16]. We calculate the free energy  $[F]_{\text{av}} = -k_B T [\ln Z]_{\text{av}}$  averaged over the random bond interaction  $b_{ij}$  with probability distribution Eq. (6), where  $[\ ]_{\text{av}}$  means the average over  $b_{ij}$  and  $Z$  is the canonical partition function. To avoid the difficulty of taking an average of  $\ln Z$ , the replica trick [6] utilizes a mathematical identity,  $\ln x = \lim_{n \rightarrow 0} (x^n - 1)/n$ . Thus,

$$-\beta [F]_{\text{av}} = [\ln Z]_{\text{av}} = \lim_{n \rightarrow 0} \frac{[Z^n]_{\text{av}} - 1}{n}. \quad (7)$$

We then concentrate on  $[Z^n]_{\text{av}}$ , which is explicitly given as

$$[Z^n]_{\text{av}} = \int \prod_{i>j} [db_{ij}P(b_{ij})] \int \prod_{\alpha=1}^n \mathcal{D}\mathbf{r}_i^\alpha e^{-\beta \sum_{\alpha} H(\{\mathbf{r}_i^\alpha\})}, \quad (8)$$

where

$$\mathcal{D}\mathbf{r}_i \equiv \prod_i d\mathbf{r}_i \delta\left(\sum_i \mathbf{r}_i\right). \quad (9)$$

The  $\delta$  function in the above equation is used to fix the center of mass at the origin. Since the integrand in Eq. (8) is a Gaussian function with respect to  $b_{ij}$ , we can integrate  $b_{ij}$  out at the beginning to get

$$[Z^n]_{\text{av}} = \int \prod_{\alpha} \mathcal{D}\mathbf{r}_i^\alpha e^{-\beta H_{\text{eff}}}. \quad (10)$$

The effective Hamiltonian here is of the form

$$H_{\text{eff}} = H_0 + H_1 + H_2, \quad (11)$$

each term of which is given as

$$\begin{aligned} H_0 &= k_B T \sum_{\alpha,i} \frac{(\mathbf{r}_{i+1}^\alpha - \mathbf{r}_i^\alpha)^2}{2a^2}, \quad (12) \\ H_1 &= \sum_{\alpha} q_{\alpha} E^T + \sum_{\alpha} \frac{v}{2} \left[ b_0 (1 - q_{\alpha}) - \frac{\beta b^2}{2} (1 - q_{\alpha})^2 \right] \\ &\quad \times \sum_{i \neq j} \delta(\mathbf{r}_i^\alpha - \mathbf{r}_j^\alpha) + c \frac{v^2}{6} \sum_{\alpha} (1 - q_{\alpha}) \\ &\quad \times \sum_{i \neq j \neq k} \delta(\mathbf{r}_i^\alpha - \mathbf{r}_j^\alpha) \delta(\mathbf{r}_j^\alpha - \mathbf{r}_k^\alpha) \quad (13) \end{aligned}$$

and

$$\begin{aligned} H_2 &= -\frac{\beta b^2 v^2}{4} \sum_{\alpha \neq \beta} (1 - q_{\alpha})(1 - q_{\beta}) \\ &\quad \times \sum_{i \neq j} \delta(\mathbf{r}_i^\alpha - \mathbf{r}_j^\alpha) \delta(\mathbf{r}_i^\beta - \mathbf{r}_j^\beta). \quad (14) \end{aligned}$$

$H_0$  maintains the polymeric chain connectivity,  $H_1$  includes the one-replica part, and  $H_2$  represents the inter-replica interaction. Obviously, the latter term is the driving force of the RSB.

Integration over the vast configuration space in Eq. (10) is too complicated to execute exactly. So, we generalize the variational principle well-known in the statistical physics [34] to replica space; For any reference Hamiltonian  $H_{\text{ref}}(\{\mathbf{r}_i^\alpha\})$ , we have an inequality relation,

$$F_{\text{var}} \equiv F_{\text{ref}} + \langle H_{\text{eff}} - H_{\text{ref}} \rangle \geq F_{\text{eff}}, \quad (15)$$

where

$$-\beta F_{\text{ref}} = \ln Z_{\text{ref}} = \ln \int \prod_{\alpha} \mathcal{D}\mathbf{r}_i^\alpha e^{-\beta H_{\text{ref}}},$$

$-\beta F_{\text{eff}} = \ln[Z^n]_{\text{av}}$  and  $\langle \dots \rangle$  means an expectation value for the Hamiltonian  $H_{\text{ref}}$ . This inequality holds before we take a

limit  $n \rightarrow 0$ . Using this principle we optimize  $F_{\text{var}}$  with respect to order parameters included in the reference Hamiltonian. With the optimized  $F_{\text{var}}^*$ , we get an estimate of the free energy we are seeking,  $[F]_{\text{av}} = \lim_{n \rightarrow 0} F_{\text{eff}}/n \simeq \lim_{n \rightarrow 0} F_{\text{var}}^*/n$ .

Reference trial functions need to be simple enough to lead to a soluble partition function but flexible enough to include order parameters which characterize all relevant phase transitions. The coil-globule transition, the folding transition, and the glass transition can be characterized by the radius of gyration, by a fluctuation scale around the native structure, and by an inter-replica correlation (Debye-Waller factor in the glass phase), respectively. A natural choice for a reference Hamiltonian is

$$\begin{aligned} \beta H_{\text{ref}} &= A \sum_{\alpha,i} (\mathbf{r}_{i+1}^\alpha - \mathbf{r}_i^\alpha)^2 + B \sum_{\alpha,i} (\mathbf{r}_i^\alpha)^2 + C \sum_{\alpha,i} (\mathbf{r}_i^\alpha - \mathbf{r}_i^T)^2 \\ &\quad + D \sum_{\alpha \neq \beta, i} d_{\alpha\beta} (\mathbf{r}_i^\alpha - \mathbf{r}_i^\beta)^2, \quad (16) \end{aligned}$$

where  $A = (2a^2)^{-1}$  and all  $B$ ,  $C$ ,  $D$ , and  $d_{\alpha\beta}$  are free parameters to be optimized based on the variational principle Eq. (15). Once these parameters are optimized, they play the role of the global order parameters;  $B$ ,  $C$ ,  $D$ , and  $d_{\alpha\beta}$  represents the radius of gyration, fluctuation around the native structure, inter-replica correlation, and the mode of RSB, respectively.

As for the mode of RSB, we rely on analogy to the Potts glass with components more than 4. As we mentioned, many other models exhibit the same type of RSB and this is believed to be quite universal for the system without inversion symmetry. In this class of systems, one level of Parisi's RSB scheme has been shown to be sufficient to describe the stable and metastable states [29] and we concentrate on this level of description in this paper. Then,  $n$  replicas are divided into  $n/m$  groups, each of which has size  $m$  and the matrix element  $d_{\alpha\beta}$  is 1 if  $\alpha$  and  $\beta$  ( $\alpha \neq \beta$ ) belong to the same group and 0 otherwise.

### C. Free energy

We just give an overview of the derivation and the expression for the variational free energy  $F_{\text{var}}$  defined in Eq. (15) here. Detailed expressions may be found in the Appendix for completeness since these are not important to understand the present arguments. Physically, the free energy  $F_{\text{var}}$  consists of three parts, a conformational entropy term  $-nTS$ , a one-replica part  $\langle H_1 \rangle$  that contains the coherent part of the interactions, which ultimately give a folding funnel as well as an effective homopolymer term, and the inter-replica term  $\langle H_2 \rangle$ , which is responsible for the random interaction between monomers. We explain each of them.

In order to carry out the variational procedure we start with the calculation of  $Z_{\text{ref}}$ , which is the same as that of Sasai and Wolynes [16]. More details can be found in [16]. We first diagonalize  $d_{\alpha\beta}$  with respect to the replica index. Concentrating on each block of size  $m$ , we get two type of eigenmodes, a symmetric mode with the eigenvalue  $\Lambda_+ = 0$  (we call + mode) and  $m-1$  degenerate asymmetric modes with the eigenvalue  $\Lambda_- = 2m$  (- mode). With the diagonalized replica index  $\mu$ , we see that the integrand is just a

Gaussian function of  $\mathbf{r}_i^\mu$ . The exponent is of the form  $A \sum_{\mu ij} \mathbf{r}_i^\mu \mathcal{H}_{ij}^\mu \mathbf{r}_j^\mu$ , where the coefficient matrix  $\mathcal{H}^\mu$  ( $\mu = \pm$ ) is

$$\mathcal{H}^\pm = \begin{pmatrix} 2 \cosh \lambda_\pm - 1 & -1 & 0 & 0 & \cdots & 0 \\ -1 & 2 \cosh \lambda_\pm & -1 & 0 & \cdots & 0 \\ 0 & -1 & 2 \cosh \lambda_\pm & -1 & \cdots & 0 \\ & & & \cdots & & \\ & & & \cdots & -1 & 2 \cosh \lambda_\pm & -1 \\ & & & \cdots & 0 & -1 & 2 \cosh \lambda_\pm - 1 \end{pmatrix},$$

where  $\lambda_\pm$  is defined by  $2 \cosh \lambda_\pm = 2 + (B + C + \Lambda_\pm D)/A$ . Thus, it is straightforward, although complicated, to integrate over configuration space and the result is represented in terms of  $G_{ij}^\pm$ , the inverse matrix of  $\mathcal{H}^\pm$ .  $F_{\text{ref}}$  is given as a function of  $B, C, D$ , and  $m$ , the explicit formula of which is given in the Appendix.

The conformational entropy  $S$  is expressed by

$$nTS = -F_{\text{ref}} + \langle H_{\text{ref}} \rangle - \langle H_0 \rangle. \quad (17)$$

First,  $F_{\text{ref}}$  is simply obtained as  $\beta F_{\text{ref}} = -\ln Z_{\text{ref}}$ . Second,  $\langle H_{\text{ref}} \rangle$  can be evaluated from the scaling argument. If we scale as  $\mathbf{r}_i \rightarrow \sqrt{z} \mathbf{r}'_i$ , the exponent of the integrand changes  $\beta H_{\text{ref}}(\mathbf{r}_i) \rightarrow z \beta H_{\text{ref}}(\mathbf{r}'_i)$  because  $H_{\text{ref}}$  is a homogeneous quadratic function of  $\mathbf{r}_i$ . Thus, taking a derivative of  $\ln Z_{\text{ref}}$  written in terms of  $\mathbf{r}'_i$  with respect to  $z$  we get an expression for  $\langle H_{\text{ref}} \rangle$ . Finally,  $\langle H_0 \rangle$  is simply given by  $\langle H_0 \rangle = -k_B T A (\partial \ln Z_{\text{ref}} / \partial A)$ . The conformational entropy  $S$  expressed thus in terms of order parameters  $B, C, D$ , and  $m$  is explicitly written in the Appendix.

For the estimate of  $\langle H_1 \rangle$ , we introduce an additional approximation in the spirit of the mean field theory. Defining the monomer density  $\rho_\alpha(\mathbf{r})$  as  $\rho_\alpha(\mathbf{r}) \equiv \sum_i \delta(\mathbf{r} - \mathbf{r}_i^\alpha)$ , replacing the expectation value of products by the products of expectation values (mean-field approximation), we get

$$\begin{aligned} \langle H_1 \rangle &\approx \sum_\alpha \langle q_\alpha \rangle E^T + \sum_\alpha \frac{v}{2} \left[ b_0 (1 - \langle q_\alpha \rangle) - \frac{\beta b^2}{2} (1 - \langle q_\alpha \rangle)^2 \right] \\ &\times \int \langle \rho_\alpha(\mathbf{r}) \rangle^2 d\mathbf{r} + c \frac{v^2}{6} \sum_\alpha (1 - \langle q_\alpha \rangle) \int \langle \rho_\alpha(\mathbf{r}) \rangle^3 d\mathbf{r}. \end{aligned} \quad (18)$$

In the same way, introducing the overlap order parameter function

$$Q_{\alpha\beta}(\mathbf{r}_1, \mathbf{r}_2) = \sum_i \delta(\mathbf{r}_1 - \mathbf{r}_i^\alpha) \delta(\mathbf{r}_2 - \mathbf{r}_i^\beta),$$

we can express  $H_2$  as

$$\begin{aligned} \langle H_2 \rangle &\approx -\frac{\beta b^2 v^2}{4} \sum_{\alpha \neq \beta} (1 - \langle q_\alpha \rangle) (1 - \langle q_\beta \rangle) \\ &\times \int \int d\mathbf{r}_1 d\mathbf{r}_2 \langle Q_{\alpha\beta}(\mathbf{r}_1, \mathbf{r}_2) \rangle^2. \end{aligned} \quad (19)$$

$\langle \rho_\alpha \rangle$ ,  $\langle q \rangle$ , and  $\langle Q_{\alpha\beta} \rangle$  can be calculated by direct integration and are expressed in terms of  $B, C, D$ , and  $m$ , which are given in the Appendix. We note that it is possible to calculate  $\langle H_1 \rangle$  and  $\langle H_2 \rangle$  without introducing these approximations; the result becomes more complex but does not change the argument discussed in this paper. Therefore, we employ this approximation to get simpler expressions keeping the qualitative results unchanged. It is also advantageous to use these approximations in that it makes it easy to compare our results with those of Shakhnovich and Gutin [15].

### III. COIL, GLOBULE, GLASS, AND FOLDED PHASES

Although the above results are quite general, it is hard to grasp the physical picture directly from them without any numerical work. Therefore, we introduce several other approximations to get simple analytical expressions for free energy. We take a sort of self-consistent strategy in the following way. First, we assume for each phase that one specific order parameter (or  $A$ ) is much larger than the others. Second, using this inequality, we obtain an asymptotic expression for the free energy and seek the stationary solution with respect to order parameters for each phase. Finally, we confirm that the solution indeed satisfies the inequality we assumed.

The first approximation introduced is that  $N \gg 1$  and most of the nonextensive terms are ignored. This may actually be a severe approximation for practical work since proteins are mesoscopic and possess a considerable surface area. Next, we employ the simplest description of monomer density, the so-called volume approximation [32,33];  $\langle \rho(\mathbf{r}) \rangle$  is a positive constant  $\rho$  inside the polymer and is zero outside. Thus,  $\int \rho^x(\mathbf{r}) d\mathbf{r} = V \rho^x = N \rho^{x-1}$ , where  $V$  is the total volume of the polymer and  $x$  is an integer. Thirdly, we approximate  $\int \langle Q_{\alpha\beta} \rangle^2 d\mathbf{r}_1 d\mathbf{r}_2$  as (see the Appendix)

$$\int Q_{\alpha\beta}^2 d\mathbf{r}_1 d\mathbf{r}_2 \approx N \rho \left( \frac{4\pi G_{ii}^-}{A} \right)^{-3/2}$$

(hereafter, we drop  $\langle \dots \rangle$  for simplicity) for the case  $\alpha$  and  $\beta$  belonging to the same group of one-level RSB. For the other cases,  $G_{ii}^-$  is replaced by  $g_i \equiv 1/m [G_{ii}^+ + (m-1)G_{ii}^-]$ . The other approximations we use are dependent on the phase we consider and will be explained below one by one.

### A. Coil and globule phases

The coil and globule phases may be characterized by the inequality  $A \gg B, C, 2mD$ . Assuming this inequality, we consider the radius of gyration defined by

$$R = \sqrt{\left\langle \sum_{\alpha, i} \mathbf{r}_i^{\alpha 2} \right\rangle} / nN, \quad (20)$$

and we get an asymptotic expression,

$$R^2 = \frac{3}{4} \left[ \frac{1}{m} \frac{1}{\sqrt{A(B+C)}} + \frac{m-1}{m} \frac{1}{\sqrt{A(B+C+2mD)}} \right].$$

Random-coil state should have the radius  $R \sim N^{1/2}a$ . Combining it with the above equation we see that  $B+C$  and  $2mD$  are at most of order  $N^{-2}A$ , which is consistent with the inequality we assumed. In the same way, the radius scales as  $R \sim N^{1/3}a$  in the globule phase, which leads us to the estimate  $B+C \sim N^{-4/3}A$  and  $2mD \sim N^{-4/3}A$ . Approximating that the polymer is roughly spherical with radius  $R$ ,  $\rho$  can be related to  $R$  by

$$\rho = \frac{N}{(4/3)\pi R^3}.$$

An estimate of the free energy is quite straightforward. First, starting from the full expression given in the Appendix, we can derive an asymptotic expression for the entropic part,

$$-TS = \frac{3}{4} Nk_B T \left[ \frac{1}{m} \sqrt{\frac{B+C}{A}} + \frac{m-1}{m} \sqrt{\frac{B+C+2mD}{A}} \right],$$

which is of order  $O(N^0)$  for the coil state and is  $O(N^{1/3})$  for the globule state. Second, the inter-replica term  $H_2$  is of order  $O(N^{-1/2})$  for the coil state and  $O(N^0)$  for the globule state and thus is negligible.

For convenience, we change the independent variables from  $B$ ,  $C$ , and  $2mD$  to  $\rho$ ,  $q$ , and  $2mD$ . Then, we can easily optimize  $2mD$  and  $q$  to get the solution  $2mD = q = 0$  (under some conditions discussed below), which leads to

$$R^2 = \frac{3}{4} \frac{1}{\sqrt{A(B+C)}} = \left( \frac{3N}{4\pi\rho} \right)^{2/3}$$

and

$$-TS = \frac{3}{4} Nk_B T \sqrt{\frac{B+C}{A}} \propto N^{1/3} k_B T \rho^{2/3}.$$

The latter is of order  $O(N^0)$  for the coil state and  $O(N^{1/3})$  for the globule state.

Thus, the free energy can be represented only as a function of  $\rho$  as

$$F_{CG} = N \frac{v}{2} \left( b_0 - \frac{\beta b^2}{2} \right) \rho + Nc \frac{v^2}{6} \rho^2 + N^{1/3} p \rho^{2/3} k_B T / A, \quad (21)$$

where  $[\dots]_{av}$  in the left-hand side (LHS) is dropped for simplicity and  $p$  is a constant of order unity, the value itself  $(9/16)(4\pi/3)^{2/3}$  is not important for the present purpose. The first two terms are of the form of virial expansion with co-

efficients  $b_0 - \beta b^2/2$  and  $c$ ; the random interaction induces an effective attraction proportional to  $1/T$ . The third term comes from entropy loss due to packing. Although the latter is nonextensive and is not important for many situations, we retain it because it will play important roles for some cases, as will be explained below.

### B. Glass phase

Since the glass phase is characterized by small thermal fluctuations around individual minima, we assume  $2mD \gg A \gg B, C$ . Using this relation we can straightforwardly obtain the asymptotic expression for the entropic contribution to the free energy as [16],

$$-TS = \frac{m-1}{m} Nk_B T \left[ \ln \left( \frac{2mD}{A} \right)^{3/2} - \frac{3}{2} \right].$$

This can be interpreted as a confinement entropy.

Next, let us consider the random interaction part  $H_2$ .  $G_{ii}^-$  behaves as  $A/(2mD)$  in the present limit and we have  $\int Q_{\alpha\beta}^2 d\mathbf{r}_1 d\mathbf{r}_2 \approx N\rho(4\pi)^{-3/2}(2mD)^{3/2}$ , because the cases  $\alpha$  and  $\beta$  belong to the same group of RSB and  $\sim 0$  otherwise. Here, we have to take care of the finiteness of spatial resolution as mentioned before. The above estimate holds only when  $|\mathbf{r}_1 - \mathbf{r}_2| \sim G_{ii}^-/A$  is of order  $v^{1/3}$  or larger. Otherwise,  $Q_{\alpha\beta}$  should be replaced by the  $\delta$  function with  $\delta(\mathbf{0}) = v^{-1}$ , which gives  $\int Q_{\alpha\beta}^2 d\mathbf{r}_1 d\mathbf{r}_2 \approx N\rho v^{-1}$ . To make the expression continuous with respect to the order parameter  $D$ , we switch two expressions when both take the same value. In summary,

$$\int Q_{\alpha\beta}^2 d\mathbf{r}_1 d\mathbf{r}_2 \approx \begin{cases} (4\pi)^{-3/2} N\rho(2mD)^{3/2} & \text{if } (2mD)^{3/2} \leq (4\pi)^{3/2}/v \\ N\rho v^{-1} & \text{otherwise.} \end{cases}$$

In the same way as above, we change independent variables from  $B$ ,  $C$ ,  $D$ , and  $m$  to  $\rho$ ,  $q$ ,  $2mD$ , and  $m$ . We can show that  $q=0$  is stable unless the stability gap is too large and thus we can write down the free energy expression,

$$F_{\text{glass}} = N \frac{v}{2} \left( b_0 - \frac{\beta b^2}{2} \right) \rho + Nc \frac{v^2}{6} \rho^2 - N \frac{\beta b^2 v^2}{4} (m-1) \times \begin{cases} (4\pi)^{-3/2} \rho(2mD)^{3/2} \\ \rho v^{-1} \end{cases} + N \frac{m-1}{m} k_B T \left[ \ln \left( \frac{2mD}{A} \right)^{3/2} - \frac{3}{2} \right], \quad (22)$$

where the upper (lower) term is taken when  $(2mD)^{3/2}$  is smaller (larger) than  $(4\pi)^{3/2}/v$ . The first two terms are those of virial expansion as above, the third term represents inter-replica interaction and is the driving force for the RSB, and the last term is obviously entropic.

### C. Folded phase

The folded phase is characterized by a large  $C$ , i.e., small fluctuations around an ideal native structure and so we assume  $C \gg A, B, 2mD$ . We can easily obtain an asymptotic

expression for the entropic part, as was done in [16];  $-TS \approx (3/2)Nk_B T \ln(C/A)$ . The inter-replica part  $H_2$  has the replica-symmetric contribution,  $\int Q_{\alpha\beta}^2 d\mathbf{r}_1 d\mathbf{r}_2 = (2\pi)^{-3/2} N \rho C^{3/2}$  for any pair of  $\alpha$  and  $\beta$ . Nativeness  $q$  in this limit is obtained as  $q \approx v(C/\pi)^{3/2}$ . Using this we change independent variables from  $B$ ,  $C$ , and  $D$  to  $\rho$ ,  $q$ , and  $2mD$ .

We can show that  $2mD=0$  is the stable solution and thus

$$F_{\text{folded}} = N \frac{v}{2} \left[ b_0(1-q) - \frac{\beta b^2}{2}(1-q)^2 \right] \rho + Nc \frac{v^2}{6}(1-q)\rho^2 \\ + qE^T + Nk_B T \ln \left[ \left( \frac{\pi}{A} \right)^{3/2} \frac{q}{v} \right] \\ + N \frac{\rho v \beta b^2}{4} 2^{-3/2} q(1-q)^2, \quad (23)$$

where  $q \sim 1$ . The first two terms, as is usual, have the form of a virial expansion, the third and fourth terms represent the enthalpy and entropy change due to folding, respectively. The last term, coming from inter-replica interaction, tends to cancel out the effective attraction due to the randomness appeared in the first term because protein does not feel randomness when it precisely coincides with the native structure.

In summary, Eqs. (21), (22), and (23) are the expressions for the free energy for all relevant phases, which will be used in the next sections.

#### IV. PHASE TRANSITIONS AND FREE ENERGY LANDSCAPE

Since we have obtained simple enough expressions for the free energies of several phases, we can now discuss the ‘‘phase transitions’’ for finite systems. Our emphasis is on the description of ruggedness of the free energy landscape. It has been argued repeatedly that there are a number of minima in the glass phase. We emphasize here, however, that even above the (static) glass transition temperature the appropriate free energy landscape has many minima which affect folding kinetics drastically.

##### A. Coil-globule transition (collapse)

We first discuss the coil-globule phase transition based on the free energy expression Eq. (21) as a function of density  $\rho$  ( $\rho \geq 0$ ). First of all, we ignore the third term, which is smaller in  $N$ . Then, the lowest free energy is attained at the  $\rho^* = 0$  when  $b_{\text{eff}} \equiv b_0 - \beta b^2/2 > 0$ , while it becomes positive,

$$\rho^* = -\frac{3}{2cv} \left( b_0 - \frac{\beta b^2}{2} \right) \quad (24)$$

when  $b_{\text{eff}} < 0$ . Thus, the phase transition temperature  $T_{\text{CG}}$  is determined by

$$b_0 - \frac{\beta_{\text{CG}} b^2}{2} = 0, \quad (25)$$

where  $\beta_{\text{CG}} = 1/(k_B T_{\text{CG}})$ . The third term in the free energy (21) does not change this temperature significantly for sufficiently large polymer. There are two cases, however, where

the third term plays roles. First, for a short polymer at high temperature, the third term becomes dominant; this term makes the globule state unstable and so the random-coil phase always appears in the limit of high temperature. Second, in the vicinity of  $\rho = 0$ , the third term is the largest and thus  $\partial F / \partial \rho|_{\rho=0}$  is positive infinite and so the transition is first order with very small barrier  $O(N^{-1})$ . We should mention that extending the argument to include a nonuniform description of the polymer leads us to a surface term of order  $O(N^{2/3})$  [32], which is not taken into account here. The third term here is  $O(N^{1/3})$ , which is smaller than the surface term and so the reasoning leading to the first order phase transition given here might not be appropriate. In any case, the coil-globule transition is a first order phase transition with a very small barrier and because of this it might be recognized as a second-order-like transition by numerical simulations, or in the laboratory.

##### B. Globule-glass transition

Next, we discuss the glass transition. First of all, we fix  $\rho$  at  $\rho^*$  given in Eq. (24) [15]. Roughly,  $\rho^*$  should not change significantly after the collapse although, rigorously speaking,  $\rho$  should be optimized simultaneously with the other order parameters. Here, we should remember that our starting point was based on the virial expansion, which is not very accurate in any collapsed phase. Thus we feel that the virial approach will overemphasize density variations.  $\rho^*$  in the virial approximation changes too rapidly with the other thermodynamic parameters, which would be the case for a more accurate homopolymer equation of states. Therefore, it is better to fix  $\rho^*$  by choosing  $c$  appropriately at this level of description. In other words, we change from the independent parameter  $c$  to  $\rho^*$ . Qualitative features do not change very much by this prescription. Again this will be a most accurate description when strong collapse is favored by the homopolymeric part of the pair interactions.

We seek the saddle solutions of  $F_{\text{glass}}(m, X)$  [i.e., Eq. (22)] with respect to  $m$  and  $X \equiv (2mD)^{3/2}$ . First, let us minimize  $F_{\text{glass}}/(m-1)$  with respect to  $X$ . Forgetting the first two terms which are constant in  $X$ , we have two relevant terms which have opposite effects. The third term, the driving force to stabilize the replica symmetry breaking solution, tends to push  $X$  to its maximum value  $X_{\text{max}} = (4\pi)^{3/2} v^{-1}$ . See Fig. 2, in which a dotted line with ‘‘ $T \ln X$ ’’ corresponds to the third term. On the other hand, the fourth term, the entropy loss due to freezing, prefers small  $X$  (another dotted line with ‘‘ $-\beta X$ ’’ in Fig. 2). At sufficiently high temperature, the fourth term, which is proportional to  $T$ , always dominates and so  $X=0$  is the only stable solution, as is illustrated in the figure. At decreasing temperature, the third term, which is inverse proportional to  $T$ , becomes important at large  $X$  and, in addition to the solution  $X=0$ , a new solution  $X=X_{\text{max}}$  becomes locally stable when

$$\left. \frac{\partial F_{\text{glass}}}{\partial X} \right|_{X=X_{\text{max}}} = 0, \quad (26)$$

which gives

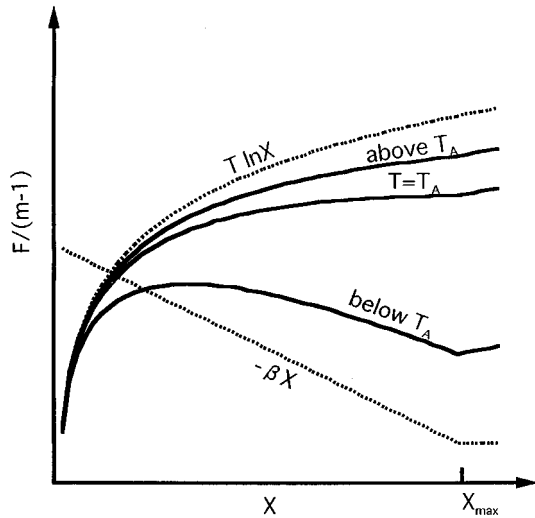


FIG. 2. The free energy as a function of  $X=(2mD)^{3/2}$ . The dotted curve with “ $T \ln X$ ” represents the third term of Eq. (22) and the dotted curve with “ $-\beta X$ ” corresponds to the fourth term. Three solid curves represent the sum of them for different temperatures.  $T=T_A$  is the critical temperature below which there is a minimum at  $X=X_{\max}$ .

$$\frac{\beta^2 b^2 \rho^* v m}{4} = 1. \quad (27)$$

We call this critical temperature  $T_A$  following [23]. For structural and Potts spin glasses this is the transition temperature predicted by mode coupling theory [21]. Below  $T_A$ , there are always two locally stable solutions  $X=0$  and  $X=X_{\max}$ , a melted phase and frozen phase, respectively. We should mention that Eq. (22) is derived under the assumption that  $D \gg A, B, C$ , which does not hold true for the solution  $X=0$  (i.e.,  $D=0$ ). Thus, we have to use the free energy expression for the coil-globule phase keeping a small dependence on  $D$ . We find  $X=0$  is indeed a stable solution, at the end.

Next, at  $T \leq T_A$ , we optimize

$$F(m, X_{\max}) = \frac{1}{4} N \rho^* v \left( b_0 - \frac{\beta b^2}{2} \right) - \frac{1}{4} N \rho^* v \beta b^2 (m-1) + N k_B T \frac{m-1}{m} (\ln p' \gamma - 3/2) \quad (28)$$

with respect to  $m$ , where  $p' \equiv (8\pi)^{3/2}$  and  $\gamma \equiv a^3/v$ . ( $\gamma$  represents flexibility of the chain and is about 5 for very flexible chainlike protein [32,35]. The value of  $p'$  depends to some extent on the approximations we use and thus we think its precise value is somewhat uncertain. Qualitative results are not affected by its value as long as it is of order unity. In discussing lattice model results we therefore treat it as adjustable.) In the same way as above, the second and third terms lead to effects in opposite directions (see Fig. 3). The stationarity condition,

$$\frac{\partial F_{\text{glass}}(m, X_{\max})}{\partial m} = 0, \quad (29)$$

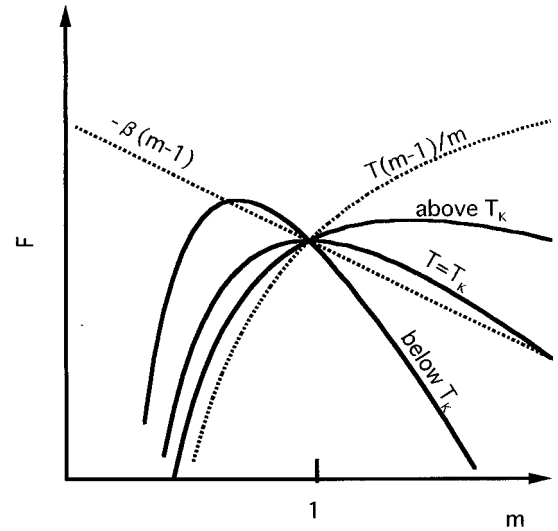


FIG. 3. The free energy as a function of  $m$ . The dotted curve with “ $T(m-1)/m$ ” represents the second term of Eq. (28) and the dotted curve with “ $-\beta(m-1)$ ” corresponds to the third term. Three solid curves represent the sum of them for different temperatures.  $T=T_K$  corresponds to the critical temperature at which  $m^*=1$ .

leads us to  $m^* = 2k_B T / b (\ln p' \gamma - 3/2 / \rho^* v)^{1/2}$ . Inserting this into Eq. (27) we get

$$k_B T_A = \frac{b}{2} \sqrt{\rho^* v (\ln p' \gamma - 3/2)}. \quad (30)$$

At  $T=T_A$ ,  $m_A^* = \ln p' \gamma - 3/2$  is larger than unity, and so in the ordinary replica formalism this solution has been ignored for the reason that it does not contribute to the Boltzmann average. Physically this means the configurational entropy of these local free energy minima is extensive at  $T_A$ . Recently, Kurchan, Parisi, and Virasoro [29] interpreted this solution as yielding the metastable states in the case of the  $p$ -spin spherical model. We follow their argument and allow  $m$  to be larger than unity. The  $m^*$  decreases linearly with  $T$  and coincides with unity at  $T=T_K$  defined by

$$k_B T_K = \frac{b}{2} \sqrt{\frac{\rho^* v}{\ln p' \gamma - 3/2}}. \quad (31)$$

Below this temperature, this frozen solution becomes dominant in the Boltzmann average. The Kauzmann temperature  $T_K$  corresponds to the case where the configurational entropy of the basins reaches zero. Equation (31) is the same as that of Shakhnovich and Gutin [15] except that the estimates of the entropy loss,  $k_B (\ln p' \gamma - 3/2)$  here, are not the same.  $T_K$  is proportional to the randomness,  $b$ , and is inversely proportional to the square root of the entropy loss, which is the same dependence found by Bryngelson and Wolynes using a statistical field version of Flory theory [8]. Moreover,  $T_K$  is proportional to the square root of  $\rho^* v$ , which represents the packing fraction. This dependence is found in [13]. (At first glance, one may notice the difference by a factor  $\sqrt{2}$  between the present result and that of Refs. [8,1]. This is simply because of the difference in the definition of randomness, as will be discussed later.)

Let us estimate the free energy at the saddle solutions. For the solution with  $X=0$ ,

$$F_{\text{globule}}^* = N \frac{v}{4} \left( b_0 - \frac{\beta b^2}{2} \right) \rho^*, \quad (32)$$

while for the solution with  $X=X_{\text{max}}$ ,

$$F_{\text{glass}}^* = N \frac{v}{4} \left( b_0 - \frac{\beta b^2}{2} \right) \rho^* - N b \sqrt{\rho^* v (\ln p' \gamma - 3/2)} \\ + N k_B T (\ln p' \gamma - 3/2) + \frac{1}{4} N \beta b^2 \rho^* v. \quad (33)$$

The energy difference between them has the simple form

$$F_{\text{glass}}^* - F_{\text{globule}}^* = (\ln p' \gamma - 3/2) N k_B T_K \left( \frac{T}{T_K} + \frac{T_K}{T} - 2 \right) \geq 0, \quad (34)$$

which touches zero at  $T=T_K$ . It should be noted that in the replica formalism the solution with the larger free energy dominates the Boltzmann average when  $m^* < 1$  as is known [6]; the solution with lower energy becomes dominant when  $m^* > 1$ . Therefore,  $F_{\text{globule}}^*$  dominates the thermal average above  $T_K$ , while  $F_{\text{glass}}^*$  becomes dominant below  $T_K$ .

Following Kurchan, Parisi, and Virasoro, we can estimate a lower bound for the free energy of transition states (TS) between the lowest local minima in the temperature range  $T_A > T > T_K$ . We conjecture that the behavior of the RSB in our model is analogous to that of the  $p$ -spin spherical model and so the TS solution is again represented by one-level RSB in the temperature range considered now. Then, the TS solution ( $m^\ddagger, X^\ddagger$ ) may be assigned to the one which makes  $F/(m-1)$  maximum with respect to  $X$  ( $X^\ddagger$  in Fig. 2). The saddle condition gives

$$2 \ln \frac{T}{T_A} - \ln \frac{m^\ddagger}{m_A^*} + m_A^* - m^\ddagger = 0 \quad (35)$$

and

$$X^\ddagger = \frac{4(k_B T)^2 (4\pi)^{3/2}}{m^\ddagger b^2 \rho^* v^2}. \quad (36)$$

The parameter  $m^\ddagger > 1$  indicates these are configurational entropy driven transitions. In general the parameter  $m < 1$  is conjugate to the nonextensive complexity of states below the thermal transition, while here  $m^\ddagger > 1$  presumably represents the fact that multiple escape routes are possible from a trapped state. The upper equation cannot be solved analytically in its general form. By the Taylor expansion around  $T_A$  ( $T \leq T_A$ ) we get

$$\Delta F^\ddagger \equiv F_{\text{glass}}^\ddagger - F_{\text{globule}}^* \\ = N k_B T_A \frac{m_A^* - 1}{m_A^* + 1} \left( \frac{T - T_A}{T_A} \right)^2 + O \left[ \left( \frac{T - T_A}{T_A} \right)^3 \right], \quad (37)$$

which clearly shows that barrier heights grow with decreasing temperature starting from zero at  $T=T_A$ . Obviously, this temperature-dependent barrier height will give a non-

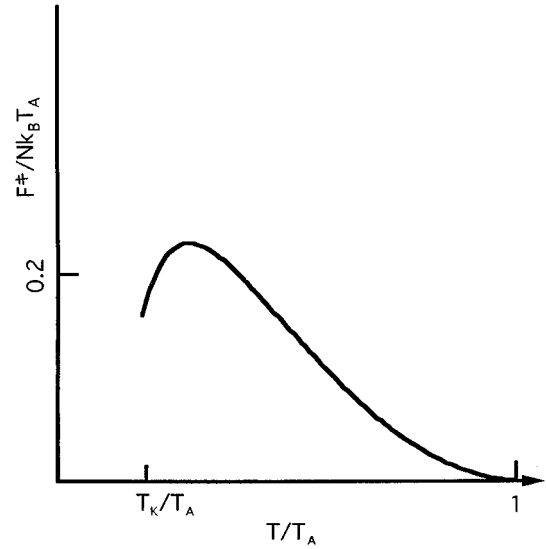


FIG. 4. The free energy barrier between the two lowest minima as a function of temperature.

Arrhenius behavior in the kinetics, as is well-known in the structural glass physics. Notice that this behavior is consistent with  $T_A$  being a sort of spinodal for the random minima.

We also show a numerical estimate of the barrier heights at  $T_A > T > T_K$  in Fig. 4. We solve Eq. (35) numerically for  $m^\ddagger$  and put it, together with Eq. (36), into Eq. (22). Here, barrier heights grow near  $T_A$  as was shown above and then start decreasing. The latter is because  $X^\ddagger$  in Eq. (36) decreases with decreasing temperature and the approximation  $2mD \gg A, B, C$  becomes worse. It is expected that real barrier heights grow monotonically. The value of the barrier height depends on the nonuniversal number  $p'$  and may not be accurate; the naive choice of  $p' = (8\pi)^{3/2}$  gives  $\Delta F^\ddagger \sim 1.0 N k_B T_K$  at around  $T_K$ , which is three times higher than that estimated from the 27-mer lattice model by simulation [36]. A smaller value  $p' = (8\pi)^{3/2}/5$  gives a comparable barrier height to the simulation  $\sim 0.4 N k_B T_K$ . We should also note that the barrier height is always proportional to the size of polymer  $N$  in the present description, which might be appropriate for relatively small proteins but is probably not accurate for larger ones, where inhomogeneous saddle points may dominate. This may also be the reason the naive estimate gives a larger barrier than the simulation. We will touch upon the latter case in Sec. V.

### C. Globule-folded transition (fast folding)

To consider the folding transition we need a free energy expression applicable in the whole range  $0 \leq q \leq 1$ . As discussed above, the entropic term in the globule phase is small and is negligible as the lowest approximation. Thus we simply interpolate the entropic term between two regimes, i.e.,  $q \sim 0$  and  $q \sim 1$ . Thus one uses a simple form [37]:

$$F_{\text{CGF}}(q) = N \frac{v}{2} \left[ b_0 (1-q) - \frac{\beta b^2}{2} (1-q)^3 \right] \rho + N c \frac{v^2}{6} (1-q) \rho^2 \\ + q E^T + N k_B T \ln(p'' \gamma q + 1), \quad (38)$$

where  $p'' = (2\pi)^{3/2}$ , the value of which should not be taken as very precise. We again fix  $\rho$  at  $\rho^*$  given by Eq. (24) by

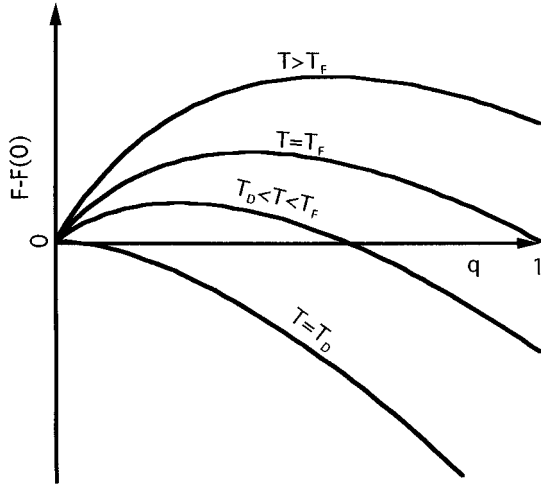


FIG. 5. The free energy as a function of nativeness  $q$  for four different temperatures. (i)  $T > T_F$ , (ii)  $T = T_F$ , the folding transition temperature, (iii)  $T_F > T > T_D$ , where folding occurs through the activation process, and (iv)  $T = T_D$  below which downhill folding takes place.

choosing  $c$  appropriately. Typical free energy curves along order parameter  $q$  are drawn in Fig. 5, which clearly shows that the folding transition is the first order. Thus, the globule-folded phase transition is defined by the relation

$$F_{\text{CGF}}(0) = F_{\text{CGF}}(1), \quad (39)$$

which now gives

$$-\frac{1}{8} \rho^* v \beta_F b^2 = -|\delta\epsilon^T| + k_B T_F \ln p'' \gamma, \quad (40)$$

where  $T_F$  is the folding temperature,  $\beta_F = 1/(k_B T_F)$ . We also defined the energy gap (per monomer)  $\delta\epsilon^T$  between the native energy and the average energy of collapsed states by

$$\delta\epsilon^T = E^T/N - \rho^* v b_0/4, \quad (41)$$

since the energy gap  $\delta\epsilon^T$  is a more useful parameter than  $E^T$  to represent the bias towards folding [38]. The LHS of Eq. (40) is the free energy of the globule, the first term in the RHS is the energy in the native state, and the second term is the entropy loss due to the folding.

The critical situation at which the free energy barrier for the folding transition disappears is determined by the relation

$$\left. \frac{\partial F_{\text{CGF}}}{\partial q} \right|_{q=0} = 0, \quad (42)$$

which now leads to  $|\delta\epsilon^T| = k_B T_D p'' \gamma + \frac{5}{8} \rho^* v \beta_D b^2$ . Here  $T_D$  is the critical temperature below which downhill folding occurs and  $\beta_D = 1/(k_B T_D)$ .

Above this critical temperature  $T_D$ , folding takes place over a free energy barrier. To think about it, we rewrite the  $q$ -dependent part of the free energy as

$$F_{\text{CGF}}/N = (\delta\epsilon^T - \frac{1}{8} \rho^* v \beta b^2) q - \frac{1}{4} \rho^* v \beta b^2 (1-q)^3 + k_B T \ln(p'' \gamma q + 1) + \text{const.}$$

The first term, mainly representing the enthalpy change due to the folding, is linearly decreasing with respect to  $q$ . On the other hand, both the second term, the effective attraction due to the randomness, and the third term, representing the entropy loss through the folding, are monotonically increasing functions of  $q$ . Therefore, the physical origin of the barrier for the folding is partly the reduction of randomness upon folding and partly the entropy loss; depending on the values of parameters, either one can be dominant. Because of this complication, the estimate of the barrier height becomes complicated too. When the barrier is small, we can write it as

$$\Delta F^\ddagger \sim N \frac{(\delta\epsilon^T + 5\rho^* v \beta b^2/8 + K_B T p'' \gamma)^2}{3\rho v \beta b^2 + 2k_B T (p'' \gamma)^2}.$$

Note that in this analysis the barrier height is always proportional to  $N$ , as in the case of the barrier between the lowest misfolded states discussed before.

#### D. Glass-folded transition

First, we fix  $\rho$  at  $\rho^*$  by eliminating  $c$  through Eq. (24), as usual. The first order phase transition between the glass phase and the folded phase is defined by

$$F_{\text{glass}}^* = F_{\text{CGF}}(1), \quad (43)$$

which now becomes

$$-|\delta\epsilon^T| + k_B T'_F \ln p'' \gamma = \frac{1}{8} \rho^* v \beta'_F b^2 - b \sqrt{\rho^* v (\ln p' \gamma - 3/2)} + k_B T'_F (\ln p' \gamma - 3/2), \quad (44)$$

where  $T'_F$  is the folding temperature from the glass phase and  $\beta'_F = 1/(k_B T'_F)$ .

### V. DISCUSSIONS

#### A. Phase diagram

Taking results in the preceding section together we can draw a few phase diagrams which are given in Fig. 6. The present model includes four independent parameters of interest, the mean value of contact energy  $b_0$ , variance of a contact interaction  $b$ , the energy gap between the native energy and the mean energy of collapsed states  $|\delta\epsilon^T|$  [defined in Eq. (41)], and temperature  $T$ , and so we have no choice but to draw a few surfaces of sections of the complete four-dimensional phase diagram. As was mentioned before, we are not taking some numerical factors  $p$ ,  $p'$ , and  $p''$  very literally at this level of description, and we use the values deduced from the lattice model, as will be explained below. A more sophisticated treatment is required to decide these values without the use of simulation data. We also note that the qualitative features of the phase diagram do not change with the choice of these parameters so long as they are of order unity.

Figure 6(a) shows a surface of section on the  $b - |\delta\epsilon^T|$  plane, which is the same representation as that of Bryngelson and Wolynes [8]. In the figure, there are three phases (bounded by solid curves), the globule phase denoted by  $M$ , the glass phase denoted by  $G$ , and the folded phase de-

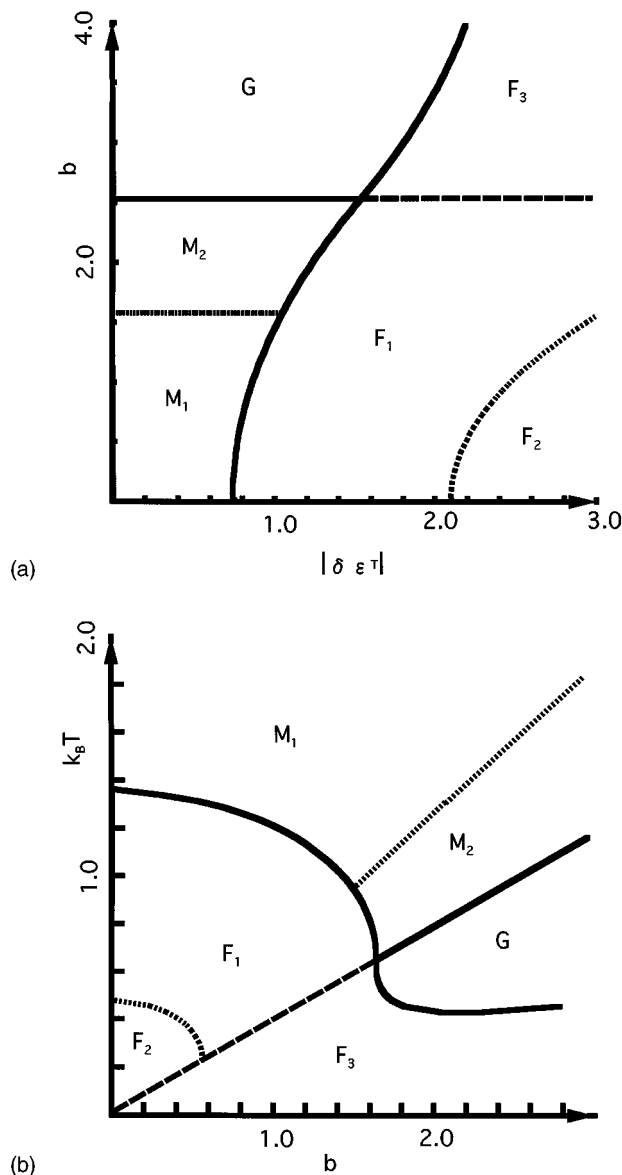


FIG. 6. Phase diagrams derived from the present model. (a) A diagram on the  $b - |\delta\epsilon T|$  plane with energy unit  $k_B T$ . (b) A diagram on the  $k_B T - b$  plane with energy unit  $|\delta\epsilon T|$ . Solid curves separate different (static) phases, dotted curves represent the boundaries at which metastable states disappear, and the dashed curve shows the glass transition in the metastable unfolded state. The  $M_1$  region is the molten globule phase with a monotonous free energy landscape. The  $M_2$  region still corresponds to the molten globule state, but the rugged free energy landscape has many minima.  $G$  denotes the glassy phase where protein misfolds to any one of the lowest states.  $F_n$  with  $n = 1, 2$ , and  $3$  is the folded phase; the  $F_1$  region has an energy barrier to folding but the system is not frozen, while there is no barrier in the  $F_2$  region.  $F_3$  corresponds to the regime where the prefolding state is glassy and thus the folding transition can be very slow. The values of the parameters used are  $\rho v = 1$ ,  $\ln p' \gamma - 3/2 = 1.6$ , and  $\ln p'' \gamma = 0.74$ , which are deduced from mapping onto the 27-mer lattice simulation.

noted by  $F$ . Roughly speaking, the phase diagram at this level is essentially the same as that of Bryngelson and Wolynes. Now, we can go forward to put in more information on the kinetics. First, the globule phase is separated into two regimes, the  $M_1$  regime, where the free energy land-

scape is monotonous and no local minimum except the globule state exists, and the  $M_2$  regime, where there are many local minima, each of which is separated by a barrier of order  $N$ , though the formal Boltzmann average is dominated by the globule state. Next, the folded phase can be separated into three parts. These are the  $F_1$  regime, where protein must pass over a free energy barrier to fold but is not trapped by the frozen state, the  $F_2$  regime, where the protein does not experience an activation barrier for the folding transition and fast downhill folding occurs, and the  $F_3$  regime, where before reaching at the folded state, the protein can be found in the glassy state and thus corresponds to a slow folding process with intermediate growth. In the recent synthesis by Bryngelson *et al.* [1], several scenarios of folding were classified. The type-0 scenario there corresponds to the  $F_2$  regime here, the type-I scenario takes place in the  $F_1$  regime, and the type-II scenario roughly corresponds to the  $F_3$  regime. For the latter case, Bryngelson *et al.* discussed the case where the glass transition takes place at the middle of the folding process, assuming that the glass transition temperature  $T_K(q)$  increases as a function of  $q$ . This seems to be the case in the lattice models studied [39]. The present analysis, however, suggests the possibility of the opposite situation, i.e., the glass transition temperature decreases as a function of  $q$  and thus there can be a case where the prefolding state is glassy, while the folded state is nonglassy. There is indeed a subtle issue whether the glass transition temperature increases or decreases as a function of  $q$  because both the ruggedness  $\Delta E^2$  and the residual entropy  $S$  decrease with respect to  $q$ . The latter quantity depends on the variational approximation used.

Figure 6(b) shows another surface of section on the  $k_B T - b$  plane (when  $b_0$  is negative). This representation corresponds to that of Sasai and Wolynes [16]. The same notation as above is used to describe each phase or regime. It is well known that the temperature dependence of folding is not simple to discuss in laboratory studies of proteins because every parameter, in principle, depends on temperature through the entropic contribution to the hydrophobic force. A similar problem occurs when comparing the phase diagram for the virial expansion Hamiltonian to a lattice model with rigid excluded volume. In order not to make the argument ambiguous, we first ignore any dependence of the parameters  $b_0$ ,  $b$ , and  $|\delta\epsilon T|$  on temperature. The phase diagram looks similar to that found by Sasai and Wolynes. One outstanding difference is that, in the present diagram, we have no random-coil phase, which appeared in Sasai and Wolynes. One reason is that we have ignored the entropic term to locate the coil-globule transition. As was mentioned, the entropic term always creates the coil phase in the high temperature limit. The other reason is related to the difference in the model itself; we assumed that all parameters are independent of  $T$  for clarity, and this is why we have no coil phase in this surface of section.

To be more realistic, we next consider the temperature dependence of the average virial coefficient  $b_0$ , which leads us to the random-coil phase in this representation. To see this, we employ the temperature dependence of  $b_0$  as

$$b_0 = \frac{T - \theta}{\theta} 2k_B T \quad (45)$$

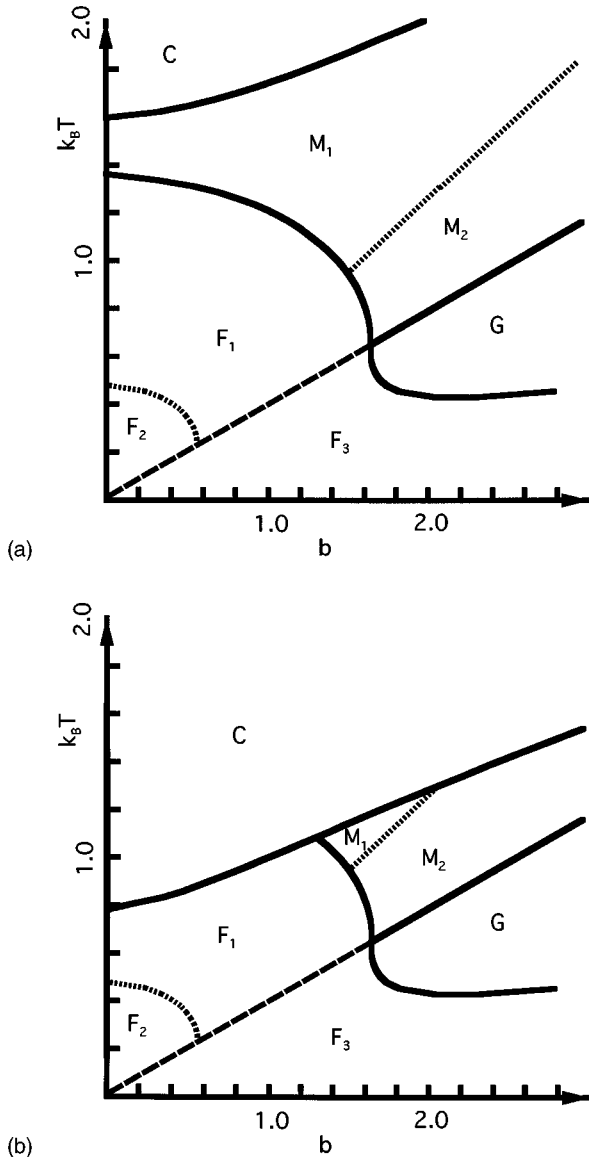


FIG. 7. Phase diagrams derived from the present model with temperature-dependent  $b_0$  defined in Eq. (45) (with energy unit  $|\delta\epsilon^T|$ ). (a) For a poorer solvent  $k_B\theta=1.0|\delta\epsilon^T|$  and (b) a better solvent  $k_B\theta=0.5|\delta\epsilon^T|$ . Notation and values of parameters used are the same as those of Fig. 6 in addition to the random-coil phase, which we denote by  $C$ .

following Grosberg and Khokhlov [32]. Here,  $\theta$  is the so-called theta temperature where  $b_0$  becomes zero. The phase diagrams for this model are given in Fig. 7 for two different values of  $\theta$ . This has the random-coil phase denoted by  $C$  as is expected and is closer to that of Sasai and Wolynes [16] as well as that of Bryngelson *et al.* [1]. For a better solvent [Fig. 7(b)], the coil phase becomes more stable and thus the coil-globule transition curve goes down. Depending on the nature of the solvent, a direct transition from the coil phase to the folded phase may also occur.

We now comment upon relations to other phase diagrams given in the literature. Shakhnovich and Gutin [15] showed a phase diagram on the  $b-b_0$  plane for the random heteropolymer. Restricting  $C\equiv 0$ , we can compare two results quantitatively. (i) The coil-globule transition curve is exactly the same. (ii) Comparing Eq. (31) with Eq. (26) of [15] we see that the only difference arises in the form of numerical

factors which are not very exact in either analysis. Next, we comment on the phase diagram given in Ramanathan and Shakhnovich [17]. Roughly speaking, the selective temperature there plays a similar role to  $b/|\delta\epsilon^T|$  here. Thus, interchanging the vertical and horizontal axes, we see that Fig. 6(b) and Fig. 1 of [17] look very similar. Socci and Onuchic drew a phase diagram based on the lattice MC simulation. Unfortunately, we cannot compare directly with their results because they fix the sequence while changing interactions between monomers, thus both  $b_0$  and  $|\delta\epsilon^T|$  depend on interactions simultaneously.

### B. Free energy landscape

We can get some insight into the ruggedness of the free energy landscape based on the analogy between the Potts-type spin glass and the present model. Figure 1 represents schematically the TAP free energy in the Potts-type spin system. This can also be viewed as a TAP free energy landscape of the random heteropolymer, although we do not present here any explicit form of TAP free energy; we can define ‘‘pure states’’ if the potential surface has many minima, each of which is separated from the others by an infinite barrier in the thermodynamic limit. An individual pure state  $s$  can be identified with the expectation value  $\{\overline{\mathbf{r}}_i^s\}$  of monomers averaged for a particular local minimum.

Referring to Fig. 1 we discuss characteristics of the free energy landscape for each temperature range. (i) At any temperature  $T$  above  $T_A$ , the landscape is monotonous and there is only one trivial solution in the TAP equation. In the replica formalism, this is represented by the replica-symmetric solution (the solution with  $D=0$ ), which corresponds to the globule state physically. (ii) At the temperature between  $T_A$  and  $T_K$ , there are both replica-symmetric and RSB solutions. The latter energy coincides with the lowest TAP free energy. To account for the formal Boltzmann average we sum over many TAP solutions as

$$Z = \int dF_{\text{TAP}} \exp[\ln\omega(F_{\text{TAP}}) - \beta F_{\text{TAP}}], \quad (46)$$

where  $\omega$  is the density of TAP solutions. In this temperature range, the exponent here has the stationary point  $F^*$  above the lowest TAP energy. Therefore, a number of TAP solutions contribute to the Boltzmann average and, due to this degeneracy (complexity), the free energy  $F = -1/\beta \ln Z$ , which coincides with the replica-symmetric free energy  $F_{\text{RS}}$ , becomes lower than the lowest TAP energy ( $=F_{\text{RSB}}$ ). For finite systems such as actual proteins, the infinitely long time behavior can be represented by the replica-symmetric solution, i.e., the globule state, while the protein nevertheless has a large barrier to move between globally different states and finite time dynamics may be controlled by the metastable RSB solution, i.e., the glassy state. Activated transport among many TAP minima takes place. (iii) Below  $T_K$ , the stationary point  $F^*$  in the exponent of Eq. (46) disappears and a few lowest minima in the free energy landscape dominate the Boltzmann average. Since the lowest TAP free energy still coincides with the RSB free energy, the glassy state becomes globally stable.

Next, we discuss the physical interpretations of  $T_A$  and  $T_K$ .  $T_K$  is the temperature where the entropy becomes zero,

sometimes called “entropy crisis.” The average number of contacts can be estimated as  $\rho^*v/2$  and variance of the random energy distribution per monomer becomes  $\Delta\epsilon^2 \sim \rho^*vb^2/2$ , while the entropy loss per monomer  $s_{\text{loss}}$  through freezing is  $k_B(\ln p' \gamma - 3/2)$ . Therefore,  $T_K$  is expressed as

$$k_B T_K = \sqrt{\frac{(\Delta\epsilon)^2}{2s_{\text{loss}}/k_B}},$$

which is consistent with the analysis of the REM [1,8]. Note that the entropy factor is in the denominator; increasing the flexibility per Kuhn segment  $\gamma$  [35], the entropy to be lost for freezing increases and then the Kauzmann temperature  $T_K$  becomes lower. On the other hand, since  $T_A$  is given by  $k_B T_A = b/2\sqrt{\rho^*v}(\ln p' \gamma - 3/2)$ , increasing the flexibility  $\gamma$ , it becomes easier to make multiple minima in the free energy landscape and thus  $T_A$  increases. As a result, a polymer with large  $\gamma$  possesses a relatively wide temperature range between  $T_A$  and  $T_K$ .

In the preceding section, we have shown that barrier heights between two lowest minima in the free energy landscape increase with decreasing temperature below  $T_A$ . This directly leads to the super-Arrhenius temperature behavior, for example, in the diffusion constant in this temperature regime. On the other hand, from the analogy to the REM [9], we expect that barrier heights saturate at  $T_K$ , below which the diffusion constant recovers the Arrhenius temperature dependence. To deal with the temperature range below  $T_K$  explicitly, following Ref. [29], we need to employ two-level RSB, which is straightforward but somewhat more elaborate.

### C. Mapping onto the 27-mer lattice model of protein

We can try to map the present model onto the three-letter code 27-mer lattice model studied exhaustively by MC simulations [39,36], although the present model is not a lattice-type one. While this mapping must be ambiguous to some extent, it is helpful in understanding the simulation results. In the lattice model [39,36], (i) the average energy of the globule state is  $-50$ , which corresponds to  $\rho v b_0/4 \leftrightarrow -50/27 = -1.8$ ; (ii) the energy of the native structure is  $-84$  and thus subtracting the average energy, we get the stability gap per monomer,  $|\delta\epsilon^T| \leftrightarrow (84 - 50)/27 = 1.3$ ; (iii) the entropy loss for freezing to a unique structure from a free chain should be roughly  $\ln 5$  for the cubic lattice giving the estimate  $k_B(\ln p' \gamma - 3/2) \leftrightarrow 1.6$ ; (iv) on the other hand, the entropy loss for the globule-folded transition was estimated as  $20k_B$  from simulation of 27-mer at the folding temperature giving a different value  $\ln p' \gamma \leftrightarrow 20/27 = 0.74$ ; (v) the measured energy fluctuation at the folding temperature is  $51$  and so  $\rho v b^2/2 \leftrightarrow 51/27 = 1.88$ . From these mappings, we can determine the dynamic glass temperature, the static glass temperature, and the folding temperature to be  $T_A = 1.23$ ,  $T_K = 0.77$ , and  $T_F = 1.25$ , respectively. On the other hand, there is no real solution for  $T_D$ ; apparently a strictly downhill scenario folding (spinodal folding) cannot be reached with these parameters.

These estimates are very crude and tentative, but it still may be interesting to discuss the folding scenario based on it. From this estimate,  $T_A$  and  $T_F$  are very close to each other

and thus usually folding occurs below  $T_F$ , so the protein encounters multiple minima along its folding route. Therefore, the most probable scenario is that, after hopping among many local minima, protein finds its native structure which is stable thermodynamically. On the other hand, because the estimates are uncertain, one should consider the possibility that folding may occur in a regime where chain dynamics is not far from Rouse dynamics renormalized by mode coupling effects [40].

We should give a warning that changes in the mapping procedure may change this assignment of the scenario to some extent. Folding is expected to occur at temperatures somewhat above  $T_K$  and thus the characteristics of the free energy landscape in this regime are of most interest. More exhaustive study of off-lattice simulation seems to be desirable to study details of the free energy landscape and kinetics. The present analytical calculation should be tested more carefully by off-lattice simulation.

Very recently, Shakhnovich and co-workers have carried out lattice simulations that suggest that random heteropolymer dynamics is not activated at high temperature [41], adducing a polynomial dependence of the time scale on system size. This would be consistent with the expectation of a mode coupling analysis about  $T_A$ , where polynomial divergences with chain length are expected [42]. At low temperatures activated dependence is seen, however. A more exhaustive version of such studies may help in quantifying  $T_A$  versus  $T_K$ .

### D. Folding kinetics: Comments on the effects of inhomogeneity

In this paper we concentrated on the case where all order parameters  $B$ ,  $C$ , and  $D$  are independent of  $i$ ; we have restricted our description to a homogeneously ordered or trapped polymer. In particular, because of this the two types of barrier heights discussed in this paper are proportional to  $N$ , which may not be appropriate for relatively large protein. For the latter, many inhomogeneous states may play important roles, especially to describe the folding kinetics. First, a folding nucleus can be represented as a state where part of the chain has much larger  $C_i$  than the other part. Nucleation [43–46] would naturally be followed by the growth of the number of monomers having larger  $C_i$ . The question addressed by such an analysis would be the size dependence of the free energy barrier for the folding transition. Second, for quite a large polymer, a specific separation of  $C_i$  into two values may create a (meta)stable state. This might be related to a foldon, a small quasi-independent folding unit [47]. Another possibility of inhomogeneous states is a locally trapped state, which means only part of the chain has large  $D_i$ , while the others have  $D_i \sim 0$ . This might be a transition state between totally frozen states and that between a frozen state and a melted state. We can extend our treatment to these inhomogeneous cases with the trial Hamiltonian,

$$\begin{aligned} \beta H_{\text{ref}} = & A \sum_{\alpha,i} (\mathbf{r}_{i+1}^\alpha - \mathbf{r}_i^\alpha)^2 + \sum_{\alpha,i} B_i (\mathbf{r}_i^\alpha)^2 + \sum_{\alpha,i} C_i (\mathbf{r}_i^\alpha - \mathbf{r}_i^T)^2 \\ & + \sum_{\alpha \neq \beta, i} D_i d_{\alpha\beta} (\mathbf{r}_i^\alpha - \mathbf{r}_i^\beta)^2. \end{aligned} \quad (47)$$

Detailed results for these problems are under study and will be reported elsewhere.

These inhomogeneous descriptions of the polymer require more elaborate modes of replica symmetry breaking. For example, in the case of the  $p$ -spin spherical model, one-level RSB is enough to represent stable states at temperature below  $T_K$ , while at the same temperature range two-level RSB describes transition states between two lowest minima [29]. Correlation of the free energy landscape has been modeled in terms of generalized REM, which includes the continuous part of Parisi's order parameter and is a step in this direction [13].

We note here that an inhomogeneous version of the analysis here gives results analogous to Kirkpatrick and Wolynes's first calculation of barriers based on a simple interface between TAP solutions [23]. Indeed Parisi [48] obtained the same dependence as KW on  $(T-T_K)$ , i.e.,  $\Delta F^\ddagger \sim (T-T_K)^{-2}$  for Potts glasses in three dimensions. Later, Kirkpatrick, Thirumalai, and Wolynes showed how wetting of the interface between two TAP solutions in a droplet by other TAP solutions led to the more usual Vogel-Fulcher behavior  $\Delta F^\ddagger \sim (T-T_K)^{-1}$  [21(b)]. This would apparently require a more complete spatially inhomogeneous RSB for the saddle point. We note that recently Thirumalai has argued, based on the KTW style argument, that barriers for traps should scale only as  $N^{1/2}$  [46]. In our view further analysis is needed because this scaling argument should be only valid in the strict vicinity of  $T_K$ , not necessarily the high temperature relevant for folding of minimally frustrated proteins.

As was noted, virial expansion used in this paper is not very appropriate to describe compact states. Incorporating rigid chain connectivity with hard core repulsion will overcome this disadvantage. In principle, Fixman's independent-oscillator comparison potential [49] might be applied to do this, although qualitative results discussed here are believed to be unchanged. The effects of the hardcore on  $T_A$  may be considerable, since even the homogeneous hard sphere fluid possesses a mean field dynamical transition. Also the somewhat subtle questions such as change in the radius of gyration from the molten-globule state to the folded state may be analyzed by this extension.

## VI. CONCLUSIONS

We have analyzed the free energy landscape of model protein based on the replica variational method. The ruggedness of free energy landscape is manifested by two glass transition temperatures,  $T_A$  and  $T_K$  ( $T_A > T_K$ ). (i) Above  $T_A$ , the landscape is monotonous. Dynamics is like that of a free Rouse chain modified by mode coupling effects. These effects would give dynamical freezing at  $T_A$ . (ii) Between  $T_A$  and  $T_K$ , the landscape has a number of metastable minima but the collection of them dominates the Boltzmann average as a whole. These are represented by the replica symmetric solution, while the RSB solution is metastable. (iii) Below  $T_K$ , only a few lowest states contribute to the Boltzmann average and this is well-described by the RSB solution. In the second regime, the barrier between the two lowest minima grows with decreasing temperature, which leads to the super-Arrhenius temperature dependence of the

diffusion constant. We believe that folding occurs somewhat above  $T_K$ , which implies a mechanism of hopping between numerous local minima until finding the native structure through the guiding forces provided by minimal frustration and the concomitant folding funnel. We have also drawn a phase diagram having seven qualitatively different dynamical regimes. Several scenarios of folding were discussed based on this diagram although it may not be quantitatively accurate in all details.

## ACKNOWLEDGMENTS

We thank Masaki Sasai and Eugene I. Shakhnovich for discussions of their results. S.T. is supported by the Japan Society for the Promotion of Science. P.G.W.'s work on folding is supported by NIH grant PHS 1 R01 GM44557.

## APPENDIX A: EXPLICIT EXPRESSIONS

Here we give explicit expressions for the variational free energy  $F_{\text{var}}$  defined in Eq. (15) in terms of parameters  $B$ ,  $C$ ,  $D$ , and  $m$  that appear in the reference Hamiltonian.

Since  $Z_{\text{ref}}$  is a many dimensional Gaussian integral with exponent  $A \sum_{\mu, ij} \mathbf{r}_i^\mu \mathcal{H}_{ij}^\mu \mathbf{r}_j^\mu$ , we can execute the integration by calculating the inverse matrix of  $\mathcal{H}^\pm$ ,

$$G_{ij}^\pm = \begin{cases} \frac{\cosh(i-1/2)\lambda_\pm \cosh(N-j+1/2)\lambda_\pm}{\sinh N \lambda_\pm \sinh \lambda_\pm}, & i < j \\ \frac{\cosh(j-1/2)\lambda_\pm \cosh(N-i+1/2)\lambda_\pm}{\sinh N \lambda_\pm \sinh \lambda_\pm}, & i \geq j \end{cases} \quad (\text{A1})$$

and the determinant, where  $\lambda_\pm$  is defined by

$$\sinh \lambda_\pm = \frac{f_\pm}{2A} \sqrt{1 + 4A/f_\pm}, \quad \cosh \lambda_\pm = 1 + \frac{f_\pm}{2A}, \quad (\text{A2})$$

where  $f_\pm = B + C + \Lambda_\pm D$  and  $\Lambda_+ = 0$ ,  $\Lambda_- = 2m$ . Using these, we can write down  $Z_{\text{ref}}$  as

$$\begin{aligned} Z_{\text{ref}} = & \left( \frac{\pi}{A} \right)^{3n(N-1)/2} N^{-3n/2} \left( \frac{\sinh \lambda_+}{\sinh N \lambda_+} \right)^{3n/2m} \\ & \times \left( \frac{\sinh \lambda_-}{\sinh N \lambda_-} \right)^{3n(m-1)/2m} \\ & \times \exp \left( \frac{nC^2}{A} \sum_{ij} \mathbf{r}_i^T G_{ij}^+ \mathbf{r}_j^T - nC \sum_i \mathbf{r}_i^{T2} \right). \end{aligned} \quad (\text{A3})$$

As was explained in Sec. II, the conformational entropy  $S$  expressed as

$$S/k_B = -\beta F_{\text{ref}} + \beta \langle H_{\text{ref}} \rangle - A \sum_{\alpha, i} \langle (\mathbf{r}_{i+1}^\alpha - \mathbf{r}_i^\alpha)^2 \rangle \quad (\text{A4})$$

can be computed directly from  $Z_{\text{ref}}$  and is written as

$$\begin{aligned} S/k_B = & \frac{3n}{2m} \left( 1 + A \frac{\partial}{\partial A} \right) \ln \frac{\sinh \lambda_+}{\sinh N \lambda_+} + \frac{3n(m-1)}{2m} \left( 1 + A \frac{\partial}{\partial A} \right) \\ & \times \ln \frac{\sinh \lambda_-}{\sinh N \lambda_-} - n \frac{C^2}{A} \sum_{ij} \mathbf{r}_i^T \left( 1 - A \frac{\partial}{\partial A} \right) G_{ij}^+ \mathbf{r}_j^T, \end{aligned} \quad (\text{A5})$$

where we dropped a trivial constant term which represents Gaussian free chain entropy.

For the one-replica part,  $\langle H_1 \rangle$  is written in terms of  $\langle \rho_\alpha \rangle$  and  $\langle q \rangle$  in the text. Thus, what we need to do here is to give expressions for the latter two quantities. The expressions for these just have an additional  $\delta$  function from the definition of  $Z_{\text{ref}}$  and are easily computed to give

$$\langle \rho(\mathbf{r}) \rangle = \sum_i \left( \frac{\pi g_i}{A} \right)^{-3/2} \exp[-A(\mathbf{r} - \mathbf{s}_i)^2/g_i], \quad (\text{A6})$$

where

$$g_i \equiv \frac{1}{m} [G_{ii}^+ + (m-1)G_{ii}^-], \quad (\text{A7})$$

$$\mathbf{s}_i \equiv \frac{C}{A} \sum_l G_{il}^+ \mathbf{r}_l^T, \quad (\text{A8})$$

and

$$\langle q \rangle = \frac{v}{N} \sum_i \left( \frac{\pi g_i}{A} \right)^{-3/2} \exp[-A(\mathbf{r}_i^T - \mathbf{s}_i)^2/g_i]. \quad (\text{A9})$$

Finally, the inter-replica term  $\langle H_2 \rangle$  is written in terms of  $\rho_\alpha$  and  $\langle Q_{\alpha\beta} \rangle$ . The latter is computed as

$$\langle Q_{\alpha\beta} \rangle = \begin{cases} \sum_i \left( \frac{\pi \tilde{g}_i}{A} \right)^{-3/2} \left( \frac{\pi G_{ii}^-}{A} \right)^{-3/2} \exp \left[ -\frac{2A}{\tilde{g}_i} \left( \frac{\mathbf{r}_1 + \mathbf{r}_2}{2} - \mathbf{s}_i \right)^2 - \frac{A}{2G_{ii}^-} (\mathbf{r}_1 - \mathbf{r}_2)^2 \right] \\ \sum_i \left( \frac{\pi g_i}{A} \right)^{-3} \exp \left[ -\frac{A}{g_i} (\mathbf{r}_1 - \mathbf{s}_i)^2 - \frac{A}{g_i} (\mathbf{r}_2 - \mathbf{s}_i)^2 \right], \end{cases} \quad (\text{A10})$$

where the upper (lower) line is for the case  $\alpha$  and  $\beta$  belong to the same (different) group of RSB and  $\tilde{g}_i$  is defined by

$$\tilde{g}_i = \frac{2}{m} G_{ii}^+ + \left( 1 - \frac{2}{m} \right) G_{ii}^-. \quad (\text{A11})$$

In the limit of large  $N$ , expressions become considerably simple. For  $G_{ij}^\pm$ ,

$$G_{ij}^\pm \approx \frac{1}{2 \sinh \lambda_\pm} \exp(-|i-j|\lambda_\pm), \quad (\text{A12})$$

which depends only on the sequential distance  $|i-j|$  between monomers. Therefore,  $G_{ii}^\pm$  is independent of  $i$  and so

$$\langle Q_{\alpha\beta} \rangle = \left( \frac{2\pi G_{ii}^-}{A} \right)^{-3/2} \exp \left[ -\frac{A}{2G_{ii}^-} (\mathbf{r}_1 - \mathbf{r}_2)^2 \right] \sum_i \left( \frac{\pi \tilde{g}_i}{2A} \right)^{-3/2} \exp \left[ -\frac{2A}{\tilde{g}_i} \left( \frac{\mathbf{r}_1 + \mathbf{r}_2}{2} - \mathbf{s}_i \right)^2 \right] \quad (\text{A13})$$

$$\sim \rho_\alpha \left( \frac{\mathbf{r}_1 + \mathbf{r}_2}{2} \right) \left( \frac{2\pi G_{ii}^-}{A} \right)^{-3/2} \exp \left[ -\frac{A}{2G_{ii}^-} (\mathbf{r}_1 - \mathbf{r}_2)^2 \right] \quad (\text{A14})$$

for the case  $\alpha$  and  $\beta$  belonging to the same group of one-level RSB, and

$$\langle Q_{\alpha\beta} \rangle = \rho_\alpha \left( \frac{\mathbf{r}_1 + \mathbf{r}_2}{2} \right) \left( \frac{\pi g_i}{A} \right)^{-3/2} \exp \left[ -\frac{A}{g_i} (\mathbf{r}_1 - \mathbf{r}_2)^2 \right] \quad (\text{A15})$$

otherwise.

- 
- [1] J. D. Bryngelson, J. N. Onuchic, N. D. Socci, and P. G. Wolynes, *Proteins: Struct. Funct. Genetics* **21**, 167 (1995).
- [2] H. S. Chan and K. A. Dill, *Phys. Today* **46** (2), 24 (1993); *Annu. Rev. Biophys. Biophys. Chem.* **20**, 447 (1991).
- [3] P. G. Wolynes, in *Spin Glasses and Biology*, edited by D. L. Stein (World Scientific, Singapore, 1992).
- [4] T. Garel, H. Orland, and D. Thirumalai, in *New Developments in Theoretical Studies of Proteins*, edited by R. Elber (World Scientific, Singapore, 1994).
- [5] C. J. Levinthal, in *Mössbauer Spectroscopy in Biological Systems*, edited by P. Debrunner, J. C. M. Tsibris, and E. Münck (Univ. of Illinois Press, Urbana, IL, 1969), p. 22.
- [6] M. Mezard, G. Parisi, and M. A. Virasoro, *Spin Glass Theory And Beyond* (World Scientific, Singapore, 1987).
- [7] P. E. Leopold, M. Montal, and J. N. Onuchic, *Proc. Natl. Acad. Sci.* **89**, 8721 (1992).
- [8] J. D. Bryngelson and P. G. Wolynes, *Proc. Natl. Acad. Sci.* **84**, 7524 (1987).
- [9] J. D. Bryngelson and P. G. Wolynes, *J. Phys. Chem.* **93**, 6902 (1989).

- [10] B. Derrida, Phys. Rev. B **24**, 2613 (1981).
- [11] W. Kauzmann, Chem. Rev. **43**, 219 (1948).
- [12] Z. Luthey-Schulten, Z. Ramirez, and P. G. Wolynes, J. Phys. Chem. **99**, 2177 (1995); J. G. Saven and P. G. Wolynes, J. Mol. Biol. **257**, 199 (1996).
- [13] S. S. Plotkin, J. Wang, and P. G. Wolynes, Phys. Rev. E **53**, 6271 (1996).
- [14] T. Garel and H. Orland, Europhys. Lett. **6**, 307 (1988).
- [15] (a) E.I. Shakhnovich and A. M. Gutin, J. Phys. A **22**, 1647 (1989); (b) Biophys. Chem. **34**, 187 (1989).
- [16] M. Sasai and P. G. Wolynes, Phys. Rev. Lett. **65**, 2740 (1990); Phys. Rev. A **46**, 7979 (1992).
- [17] S. Ramanathan and E. I. Shakhnovich, Phys. Rev. E **50**, 1303 (1994).
- [18] V. S. Pande, A. Y. Grosberg, and T. Tanaka, J. Phys. II (France) **4**, 1771 (1994).
- [19] M-H. Hao and H. A. Scheraga, J. Chem. Phys. **102**, 1334 (1995).
- [20] D. J. Gross, I. Kanter, and H. Sompolinsky, Phys. Rev. Lett. **55**, 304 (1985).
- [21] (a) T. R. Kirkpatrick and P. G. Wolynes, Phys. Rev. A **35**, 3072 (1987); (b) T. R. Kirkpatrick, D. Thirumalai, and P. G. Wolynes, *ibid.* **40**, 1045 (1989).
- [22] T. R. Kirkpatrick and D. Thirumalai, Phys. Rev. B **36**, 5388 (1987).
- [23] T. R. Kirkpatrick and P. G. Wolynes, Phys. Rev. B **36**, 8552 (1987); T. R. Kirkpatrick and D. Thirumalai, Phys. Rev. A **37**, 4439 (1988).
- [24] R. P. Feynman, Phys. Rev. **97**, 660 (1955).
- [25] M. S. Friedrichs and P. G. Wolynes, Science **246**, 371 (1989).
- [26] N. D. Socci and J. N. Onuchic, J. Chem. Phys. **101**, 1519 (1994); **103**, 4732 (1995).
- [27] A. Sali, E. I. Shakhnovich, and M. Karplus, Nature **369**, 248 (1994); J. Mol. Biol. **235**, 1614 (1994).
- [28] A. Crisanti and H-J. Sommers, Z. Phys. B. **87**, 341 (1992).
- [29] J. Kurchan, G. Parisi and M. A. Virasoro, J. Phys. I (France) **3**, 1819 (1993).
- [30] D. J. Thouless, P. W. Anderson, and R. G. Palmer, Philos. Mag. **35**, 593 (1977).
- [31] In this paper, we use an effective Gaussian chain that does not distinguish the Kuhn length from the monomer-monomer distance. Since protein is one of the more flexible polymers, this simplification may not be too crude. See, for example, [32] for more detail.
- [32] A. Y. Grosberg and A. R. Khokhlov, *Statistical Physics of Macromolecules*, translated by Y. A. Atanov (AIP Press, New York, 1994).
- [33] We note that this may be too crude, especially near the  $\theta$  temperature, where the density fluctuations are large. For this possibility, see, for example, S. S. Plotkin, J. Wang, and P. G. Wolynes [J. Chem. Phys. (to be published)]. Here we do not concentrate on the behavior near the  $\theta$  temperature but use this approximation, which is relevant when motion occurs within the ensemble of strongly collapsed states.
- [34] For example, R. P. Feynman, *Quantum Mechanics and Path Integrals* (McGraw-Hill Inc., New York, 1965).
- [35] The use of the term “flexibility” here requires caution. We first note that the Kuhn length  $a$  is of the same order as monomer-monomer distance  $l$  for the flexible chain, while  $a$  is much larger than  $l$  for the stiff chain. Thus, the stiff (flexible) chain has large (small)  $\gamma \sim 1000$  ( $\sim 5$ ). If we introduce, however, the flexibility per Kuhn segment, it takes large (small) value when  $\gamma$  is large (small) because  $\gamma$  is the number of possible states per Kuhn segment.
- [36] N. D. Socci, J. N. Onuchic, and P. G. Wolynes, J. Chem. Phys. **104**, 5860 (1996).
- [37] Here, we modified the last term in Eq. (23) based on the physical interpretation; as mentioned before, the last term is expected to cancel out the effective attraction due to the randomness in the first term of the same expression. Since we should not take the numerical coefficient too seriously in this level of calculation, we ignore the factor  $2^{-3/2}$  so that the cancellation takes place completely.
- [38] Although the quantity to be subtracted,  $\rho^* v b_0/4$ , comes from truncation of virial expansion, the gap here is a well-defined quantity within the model. We also note that what is important is basically a relative change of  $|\delta\epsilon^T|$  but not the value itself. A larger gap corresponds to a more designed sequence to the fast folding.
- [39] J. N. Onuchic, P. G. Wolynes, Z. Luthey-Schulten, and N. D. Socci, Proc. Natl. Acad. Sci. USA **92**, 3626 (1995).
- [40] K. S. Schweizer, J. Chem. Phys. **91**, 5802 (1989); **91**, 5822 (1989); J. Non-Cryst. Solids **131**, 643 (1991).
- [41] E. I. Shakhnovich, private communication at Caltech Protein Folding Meeting, 1996.
- [42] W. Götze, in *Liquids, Freezing and Glass Transition*, edited by J. P. Hansen, D. Levesque, and J. Zinn-Justin (North-Holland, Amsterdam, 1991).
- [43] J. D. Bryngelson and P. G. Wolynes, Biopolymers **30**, 177 (1990).
- [44] V. I. Abkevich, A. M. Gutin, and E. I. Shakhnovich, Biochemistry **33**, 10 026 (1994); J. Chem. Phys. **101**, 6052 (1994).
- [45] Z. Guo and D. Thirumalai, Biopolymers **36**, 83 (1995).
- [46] D. Thirumalai, J. Phys. I (France) **5**, 1457 (1995).
- [47] A. Panchenko, Z. A. Luthey-Schulten, and P. G. Wolynes, Proc. Natl. Acad. Sci. **93**, 2008 (1996).
- [48] G. Parisi (unpublished).
- [49] M. Fixman, J. Chem. Phys. **51**, 3270 (1969).
- [50] A more accurate measure of nativeness may be

$$q = v \sum_{i < j} \delta(\mathbf{r}_i - \mathbf{r}_j) \delta(\mathbf{r}_i^T - \mathbf{r}_j^T) / \sum_{i < j} \delta(\mathbf{r}_i^T - \mathbf{r}_j^T).$$

Using this definition, all the results given in this paper turn out to be the same, aside from a minor numerical factor.